Journal of Biological Systems, Vol. 17, No. 2 (2009) 319–328

TRAVELING PATTERN INDUCED BY MIGRATION IN AN EPIDEMIC MODEL

LI LI[*,‡], GUI-QUAN SUN[*,†,§] and ZHEN JIN[*,¶]
[*]*Department of Mathematics*
[†]*School of Mechatronic Engineering*
North University of China
Taiyuan, Shan'xi 030051, P. R. China
[‡]*lili831113@yahoo.com.cn*
[§]*gquansun@yahoo.com.cn*
[¶] *jinzhn@263.net*

Received 16 October 2008
Accepted 25 November 2008

The main work in spatial epidemiology is the study of spatial variation in disease risk or incidence, including the spatial patterns of the populations. Spread of diseases in human populations can exhibit different patterns for spatially explicit approaches. In this paper, we investigate an epidemic model with both diffusion and migration. In the previous work (Sun *et al., J Stat Mech* P11011, 2007), we studied the model only with diffusion and obtained stationary Turing pattern. However, combined with migration, the model will exhibit typical traveling pattern, which is shown by both mathematical analysis and numerical simulations. The results obtained well extend the finding of pattern formation in the epidemic model and may well explain the field observed in the real world.

Keywords: Epidemic Model; Migration; Traveling Pattern.

1. Introduction

Most studies concentrate on the local temporal development of diseases and epidemics. Their geographical spread is less well understood, although important progress has been achieved in many cases.[1–3] The key question, as well as difficulty, is how to include spatial effects and quantify the dispersal of individuals.[4] This problem has been studied with some effort in various ecological systems, for instance, in plant dispersal by seeds. Today's volume, speed, and nonlocality of human travel, as well as the spread of smallpox in Great Britain,[5] demonstrate that modern epidemics cannot be accounted for by local diffusion models that are applicable only as long as the mean distance traveled by individuals is small compared to geographical distances. These local reaction-diffusion models generically lead to epidemic wavefronts, which were observed, for example, in the geo-temporal

---

[¶]Corresponding author.

spread of the Black Death in Europe from 1347 to 1350.[6–8] Thus, spatial epidemic models are more suitable for describing the process of epidemiology.

One of the simplest models which captures the fundamental features of infection dynamics is the S-I (susceptible-infectious) model. Such a model exhibits a single epidemic. Each individuals can be in one of two states: susceptible to the disease, infectious who can spread the disease to susceptible. We firstly pay attention to the following reaction-diffusion model:[9]

$$\frac{\partial S}{\partial t} = rS\left(1 - \frac{S}{K}\right) - \beta S^p I^q + D_S \nabla^2 S, \tag{1a}$$

$$\frac{\partial I}{\partial t} = \beta S^p I^q - dI + D_I \nabla^2 I, \tag{1b}$$

where K represents carrying capacity, r represents intrinsic birth rate constant, β is the force of infection or the rate of transmission, d represents the death coefficient of I for the disease and D_S and D_I are the diffusion coefficients. And $\nabla^2 = \partial/\partial x^2$ or $(\partial^2/\partial x^2 + \partial^2/\partial y^2)$. For the sake of simplicity, we consider the case that $p+q=1$ and $p, q > 0$.

However, individuals can exhibit a correlated motion towards certain direction instead of random motion, and this phenomena widely exists in the real world.[11] For example, some people want to travel, study or settle down in Canada from their native country. Then they may exhibit a correlated motion from their native country towards the country where they want to go. Here, we call this phenomenon as migration. And this phenomenon can enhance the spread of some disease, such as Tuberculosis.[10] To the best of our knowledge, there is little work on the dynamical behavior of both migration and diffusion in the epidemic model. For the above reasons, in the present paper, we pose the equation to describe the spatiotemporal epidemic dynamics allowing for both migration and diffusion as follows:

$$\frac{\partial S}{\partial t} + c_S \nabla S = rS\left(1 - \frac{S}{K}\right) - \beta S^p I^q + D_S \nabla^2 S = f(S, I) + D_S \nabla^2 S, \tag{2a}$$

$$\frac{\partial I}{\partial t} + c_I \nabla I = \beta S^p I^q - dI + D_I \nabla^2 I = g(S, I) + D_I \nabla^2 I, \tag{2b}$$

where $\nabla = \partial/\partial x$ (or $\partial/\partial x + \partial/\partial y$) and c_i $(i = S, I)$ is the migration coefficient.

2. Linear Stability Analysis

The first step in analyzing the model (2) is to determine the behavior of the non-spatial model obtained by setting space derivatives equal to zero. The non-spatial model has at most three stationary states, which correspond to spatially homogeneous equilibria of the model, in the nonnegative quadrant: two disease-free states

$(0,0),(K,0)$ and an endemic stationary state $E^* = (S^*, I^*)$, where

$$\begin{aligned} S^* &= K\left(1 - \frac{\beta^{\frac{1}{p}}}{rd^{\frac{1-p}{p}}}\right), \\ I^* &= \left(\frac{\beta}{d}\right)^{\frac{1}{p}} S^*. \end{aligned}$$

And the condition to ensure that S^* and I^* are positive is that $r > \beta^{\frac{1}{p}}/d^{\frac{1-p}{p}}$.

From the biological point of view, we are interested in studying the stability behavior of the interior equilibrium point E^*, and the Jacobian matrix J is given by

$$J = \begin{pmatrix} \partial_S f & \partial_I f \\ \partial_S g & \partial_I g \end{pmatrix}_{(S^*,I^*)} = \begin{pmatrix} a_{11} & a_{12} \\ a_{21} & a_{22} \end{pmatrix}. \tag{3}$$

It is easy to see that model equation (2) is the form of generalized reaction-diffusion-migration model. To consider pattern formation for system (2), we should look for the dispersion relation, which gives the condition for pattern formation. Following Murray,[6] we will assume period (or zero-flux) boundary conditions and prescribed initial conditions. A symmetry breaking occurs when a homogeneous steady state solution of system (2) is linearly stable to perturbations in the absence of the diffusion and migration terms, but linearly unstable to small spatial perturbations in the presence of diffusion and migration. It is a simple matter to find the exact algebraic formulation of the dispersion relation when these equations are subject to certain boundary conditions and stability properties. Here we consider an approach based on Laplace transform methods which is convenient for finding symmetry breaking (Turing instability) conditions in the case when the systems include diffusion and migration. The Laplace transform methods are extensively used in the reaction-migration-diffusion equations including the system with fractional diffusion and fractional reaction.[12–14]

We make the following substitutions:

$$S = S^* + \overline{S}(\overrightarrow{r}, t), \tag{4}$$

and

$$I = I^* + \overline{I}(\overrightarrow{r}, t), \tag{5}$$

into the kinetic equations and assume $|\overline{S}| \ll S^*$, $|\overline{I}| \ll I^*$. Then, in the linear approximation, we have

$$\frac{\partial \overline{S}}{\partial t} + c_S \nabla \overline{S} = a_{11}\overline{S} + a_{12}\overline{I} + D_S \nabla^2 \overline{S}, \tag{6a}$$

$$\frac{\partial \overline{I}}{\partial t} + c_I \nabla \overline{I} = a_{21}\overline{S} + a_{22}\overline{I} + D_I \nabla^2 \overline{I}. \tag{6b}$$

The initial conditions are assumed as

$$\overline{S}|_{t=0} = f(\overrightarrow{r}) \tag{7}$$

and

$$\overline{I}|_{t=0} = g(\overrightarrow{r}), \tag{8}$$

where the functions $f(\overrightarrow{r})$ and $g(\overrightarrow{r})$ decay rapidly for $\overrightarrow{r} \to \pm\infty$. Following the standard approach, let us now perform a Laplace transformation of the linearized equations over the two independent variables $\overrightarrow{r}$ and t. For $\overrightarrow{r}$ we use the so-called two-sided version of the transformation. The relations for the forward and backward transforms are

$$S_{\lambda n} = \int_0^{\infty} e^{-\lambda t} dt \int_{-\infty}^{+\infty} \overline{S}(\overrightarrow{r}, t) e^{-n\overrightarrow{r}} d\overrightarrow{r} \tag{9}$$

and

$$\overline{S}(\overrightarrow{r}, t) = -\frac{1}{4\pi^2} \int_{\beta - i\infty}^{\beta + i\infty} e^{\lambda t} d\lambda \int_{-i\infty}^{i\infty} S_{\lambda n} e^{n\overrightarrow{r}} dn, \tag{10}$$

where λ and n are complex variables. And λ is the Laplace transform variable, n is the Fourier transform variable. That is to say that, $n = ik$ or (ik, il) corresponding to one- and two-dimensional space, and the wave numbers k and l are real numbers. In Eq. (10) for the backward transformation, the integration contour in the n-plane is the imaginary axis. In the λ-plane the contour is parallel to the imaginary axis and located to the right of all singularities of the integrand.

After this transformation, the kinetic equations read as

$$(\lambda - a_{11} + c_S n - D_S n^2) S_{\lambda n} - a_{12} I_{\lambda n} = F(n) \tag{11}$$

and

$$(\lambda - a_{22} + c_I n - D_I n^2) I_{\lambda n} - a_{21} S_{\lambda n} = G(n), \tag{12}$$

where $F(n)$ and $G(n)$ are the transforms of $f(\overrightarrow{r})$ and $g(\overrightarrow{r})$. To reveal the presence of an instability and disclose its character, it is sufficient to consider one variable. The temporal growth of the perturbations can now be found by inverting the Laplace transforms, which follows directly after factorizing the denominator. Then we obtain the linear stability of this state as described by the dispersion relation

$$\mathtt{D}(\lambda, n) = (\lambda - a_{22} + c_I n - D_I n^2)(\lambda - a_{11} + c_S n - D_S n^2) - a_{12} a_{21}. \tag{13}$$

If we set r as a bifurcation parameter, then analysis of Eq. (13) gives the thresholds for Hopf and Turing instabilities:[9]

$$r_H = 2d^{\frac{p-1}{p}} \beta^{\frac{1}{p}} - dp \left(\frac{\beta}{d}\right)^{\frac{1}{p}} - dp, \tag{14}$$

and

$$r_T = \left(2dp\beta^{\frac{1}{p}} - dp\beta\left(\frac{\beta}{d}\right)^{\frac{p-1}{p}} + 2k_T^2 D_I \beta^{\frac{1}{p}} - k_T^2 D_I \beta p \left(\frac{\beta}{d}\right)^{\frac{p-1}{p}} d^{\frac{p-1}{p}} - k_T^2 dp D_S d^{\frac{p-1}{p}} - k_T^4 D_S D_I\, d^{\frac{p-1}{p}}\right) \Big/ \left(d^{\frac{p-1}{p}}(k_T^2 D_I + dp)\right),$$

where $k_T^2 = \sqrt{(a_{11}a_{22} - a_{12}a_{21})/(D_S D_I)}$. In the rest of this paper, we investigate the pattern of the system (2) assuming that $r_H < r < r_T$.

The condition for a spatial mode n (in one- or two-dimensional space) is that it is unstable and thus system (2) grows into a pattern, that is $\mathrm{Re}(\lambda) > 0$. Here, we pay attention the one-dimensional space case, that is $n = ik$. The dispersion relation $\mathrm{Re}(\lambda) > 0$ is algebraically complicated, so we straightforwardly use Eq. (13) to study the numerical computation for this model. The condition for diffusion driven instability is that $\mathrm{Re}(\lambda_{\max}) > 0$ at $k = k_{\max} \neq 0$.

In the present paper, we focus on the parameter c_S and c_I, which determine the intensity of migration, and set that $r = 0.4$, $K = 1$, $p = 0.4$, $\beta = 0.5$, $d = 0.6$, $D_S = 0.1$ and $D_I = 0.5$. Note that under these values of the parameters, we obtain the stationary Turing pattern.[9] Figure 1 depicts the range of the values of k for some constant values, and the small perturbation may bring about an instability with time. From Fig. 1, we can see that the spatial pattern can occur due to the positive real parts of λ.

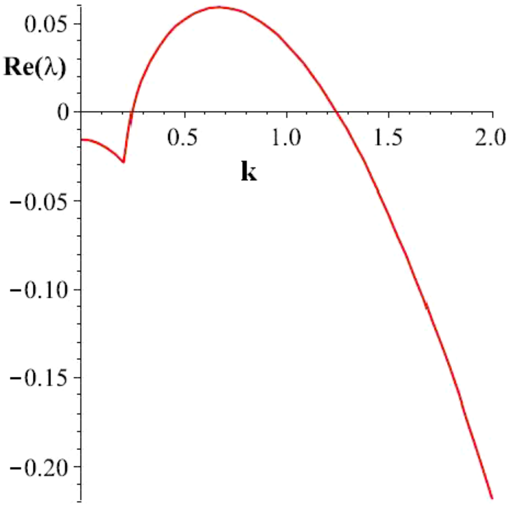

Fig. 1. An illustration of the dispersion relation [$\mathrm{Re}(\lambda)$ versus k] from the Eq. (13) with $c_S = c_I = 1$. Other parameter values are used as: $r = 0.4$, $K = 1$, $p = 0.4$, $\beta = 0.5$, $d = 0.6$, $D_S = 0.1$ and $D_I = 0.5$.

3. Main Results

In this following, we give the numerical solution to the system (2) in the one-dimensional space. We used the RK4EX algorithm for the reaction terms, a Fourier transform technique to calculate the first and second partial derivative in space x variables, i.e., the diffusion and migration terms. In addition, the Fourier technique can save the time in obtaining these results, and our numerical results also validated by using the explicit an Euler method. In our calculations, the parameters values were taken to be $\triangle x = 1, \triangle t = 0.01$ and the space was discretized to 1×100 lattices on the one-dimensional space. The periodic boundary condition was used in the simulation. Note that though we vary the number of mesh points such as 1×200 and 1×300, the quality results of system (2) are all the same. In the simulations different types of dynamics are observed and we have found that the distributions of S and I are always of the similar type.

In the previous paper,[9] we obtain the typical dynamics of population density variation is the formation of isolated groups, i.e., stripe-like or spotted or coexistence of both. Now, it is natural to ask what kind of pattern formation of the population can be observed when considering migration. It can be seen from Fig. 2 that the system (2) shows typical traveling spatial pattern when combined with migration. That is to say that, the migration term plays an important role in formation of the population, i.e., changes the Turing pattern into into traveling spatial pattern.

To well show the effect of migration, we plot the time series at some spatial point in Fig. 3. From this figure, one can conclude that migration can lead the

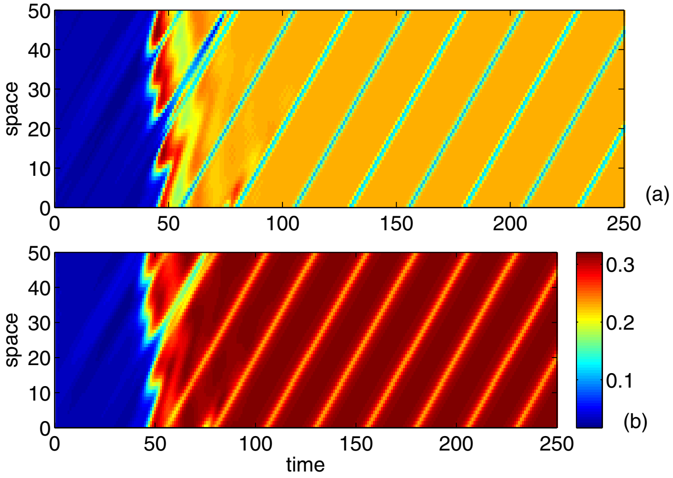

Fig. 2. Typical spatiotemporal pattern diagram for the model (2) with migration. Parameter values are used as: $r = 0.4$, $K = 1$, $p = 0.4$, $\beta = 0.5$, $d = 0.6$, $D_S = 0.1$, $D_I = 0.5$ and $c_S = c_I = 1$. (a) The pattern of the susceptible individuals; and (b) The pattern of the infectious individuals.

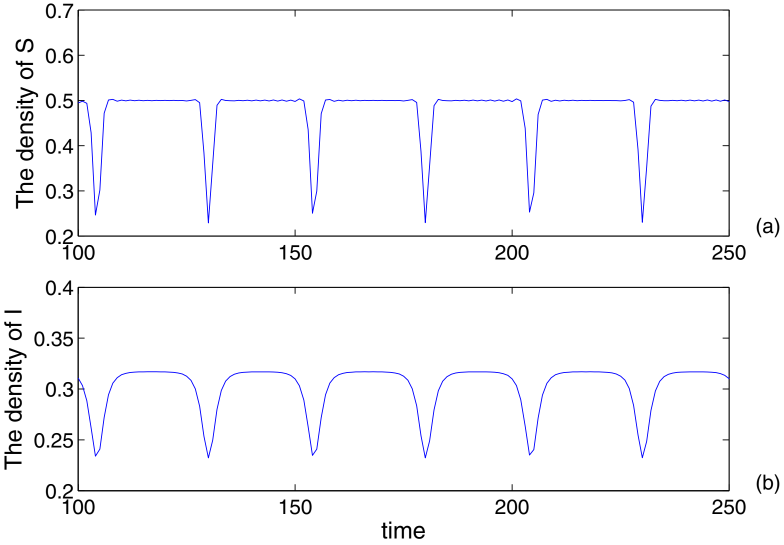

Fig. 3. Time series diagram for the model (2) with migration at $x = 25$. Parameter values are used as: $r = 0.4$, $K = 1$, $p = 0.4$, $\beta = 0.5$, $d = 0.6$, $D_S = 0.1$, $D_I = 0.5$ and $c_S = c_I = 1$. (a) The density of the susceptible; and (b) The density of the infectious.

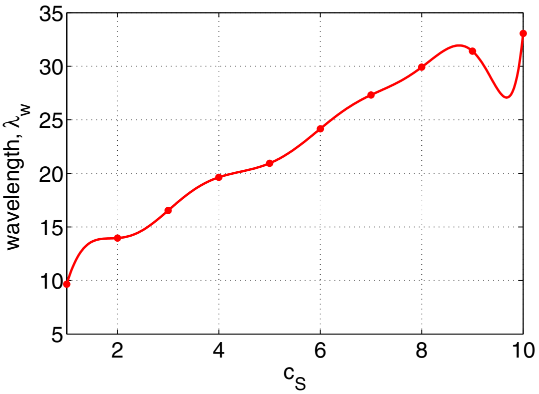

Fig. 4. An illustration of the variation in pattern wavelength with c_S. The other parameter values are the same as in Fig. 1. As shown in the figure, the wavelength increases with c_S. The wavelength is calculated using Eq. (15).

system undergoes oscillatory in time. Moreover, we find that the S and I are in synchrony at different time. The presence, absence or degree of synchronization can be an important part of the function or malfunction of a biological system. This is because synchrony may decrease the global persistence.[15] In other words, migration may lead the disease to be extinctive.

The other property that characterizes the spatial patterns of the population is wavelength. Determining the wavelength for the spatial pattern is a key issue in the field of spatial epidemiology. In other words, we can well know the distribution of the population in the spatial space by calculating the wavelength. When a spatial pattern occur, one expects that these will be dominated by the fastest growing mode. Since the fastest growing mode corresponds to the spatial pattern with wave number, $k_{\max}$, the wavelength has the following form

$$\lambda_w = \frac{2\pi}{k_{\max}}. \tag{15}$$

Combining the Eqs. (13) and (15), we can give the prediction the wavelength with respect to the parameters c_S (c_I is fixed as 1), which are shown in Fig. 4. From the figure, one can see that the wavelength is increased as c_S being increased. Biologically speaking, the migration of the population can speed up the invasion speed. This is consistent with the real world.

4. Discussion and Conclusion

We have presented a theoretical analysis of evolutionary processes that involves organism distribution and the interaction of spatially distributed populations with local diffusion and migration. Our analysis and numerical simulations reveal that the migration plays a constructive role in the pattern form, i.e., try changing the Turing pattern into traveling wave. Furthermore, we give the calculation of wavelength of the traveling pattern.

Traveling waves, arising essentially from activator-inhibitor dynamics,[16–18] are predicted by theory in a range of host-natural enemy systems.[19–22] However, even where waves are dynamically possible, they may not be detected because of a lack of spatio-temporal data at the appropriate resolution. Furthermore, few systems are documented well enough both to detect repeated waves and to explain their interaction with spatio-temporal variations in population structure and demography. In Grenfell *et al.*,[8] they demonstrate recurrent epidemic traveling waves in an exhaustive spatio-temporal data set for measles in England and Wales. Our results can well capture the main features of the observed data, which is obtained from the real world.

We illustrate the emergence of the traveling pattern in the epidemic process with the simplest dynamical description. Despite its simplicity and spatial coarseness, this model reproduces the novel phenomenon. The model is introduced in a general form so that it has broad applications to a range of interacting populations. For example, it can be applied to diseases such as measles, AIDS, flu, etc. On the other hand, recent studies show noise plays an important role on the epidemic model,[23–24] which indicates that the noise induces sustained oscillations and coherence resonance in the epidemic model. For such reason, we should pay attention to the role of noise in the future work.

Acknowledgments

This work is supported by the National Natural Science Foundation of China under Grant No. 60771026, Program for New Century Excellent Talents in University (NCET050271), the Special Scientific Research Foundation for the Subjects of Doctors in University (20060110005), and Graduate Students' Excellent Innovative Item of Shanxi Province No. 20081018.

References

1. Keeling MJ, Woolhouse MEJ, Shaw DJ, Matthews L, Chase-Topping M, Haydon DT, Cornell SJ, Kappey J, Wilesmith J, Grenfell BT, Dynamics of the 2001 UK foot and mouth epidemic: Stochastic dispersal in a heterogeneous landscape, *Science* **294**:813–817, 2001.
2. Smith DL, Lucey B, Waller LA, Childs JE, Real LA, Predicting the spatial dynamics of rabies epidemics on heterogeneous landscapes, *Proc Natl Acad Sci USA* **99**:3668–3672, 2002.
3. Keeling MJ, Woolhouse MEJ, May RM, Davies G, Grenfell BT, Modelling vaccination strategies against foot-and-mouth disease, *Nature* **421**:136–142, 2003.
4. Hufnagel L, Brockmann D, Geisel T, Forecast and control of epidemics in a globalized world, *Proc Natl Acad Sci USA* **101**:15124–15129, 2004.
5. Riley S, Ferguson NM, Smallpox transmission and control: Spatial dynamics in Great Britain, *Proc Natl Acad Sci USA* **103**:12637–12642, 2006.
6. Murray JD, Mathematical Biology, 3rd edition, Springer, Berlin, 1993.
7. Noble JV, Geographic and temporal development of plagues, *Nature* **250**:726–729, 1974.
8. Grenfell BT, Bjornstadt ON, Kappey J, Travelling waves and spatial hierarchies in measles epidemics, *Nature* **414**:716–723, 2001.
9. Sun G, Jin Z, Liu QX, Li L, Pattern formation in a spatial S-I model with non-linear incidence rates, *J Stat Mech* P11011, 2007.
10. Jia ZW, Tang GY, Jin Z, Dye C, Vlas SJ, Li XW, Feng D, Fang LQ, Zhao WJ, Cao WC, Modeling the impact of immigration on the epidemiology of tuberculosis, *Theor Pop Biol* **73**:437–448, 2008.
11. Petrovskii S, Li BL, An exactly solvable model of population dynamics with density-dependent migrations and the allee effect *Math Biosci* **186**:79–91, 2003.
12. Andresn P, Bache M, Mosekilde E, Dewel G, Borckmanns P, Stationary space-periodic structures with equal diffusion coefficients, *Phys Rev E* **60**:297–301, 1999.
13. Henry BI, Wearne SL, Existence of turing instabilities in a two-species fractional reaction-diffusion system, *SIAM J Appl Math* **62**:870–887, 2002.
14. Kuznetsov SP, Mosekilde E, Dewel G, Borckmans P, Absolute and convective instabilities in a one-dimensional brusselator flow model, *J Chem Phys* **106**:7609–7616, 1997.
15. Blasius B, Tönjes R, *Analysis and Control of Complex Nonlinear Processes in Physics, Chemistry and Biology*, World Scientific, Singapoore, 2007.
16. Neubert MG, Kot M, Lewis MA, Dispersal and pattern formation in a discrete time predator-prey model, *Theor Pop Biol* **48**:7–43, 1995.
17. Sherratt JA, Periodic travelling waves in cyclic predator-prey systems, *Ecol Lett* **4**:30–37, 2001.

18. Hassell MP, Comins HN, May RM, Spatial structure and chaos in insect population dynamics, *Nature* **353**:255–258, 1991.
19. Solé RV, Valls J, Bascompte J, Spiral waves, chaos and multiple attractors in lattice models of interacting populations, *Phys Lett A* **166**:123–128, 1992.
20. Jeltsch F, Muller MS, Grimm V, Wissel C, Brandl R, Pattern formation triggered by rare events: lessons from the spread of rabies, *Proc R Soc Lond B* **264**:495–503, 1997.
21. Bjørnstad ON, Ims RA, Lambin X, Spatial population dynamics: Causes and consequences of spatial synchrony in density fluctuations, *Trends Ecol Evol* **14**:427–431, 1999.
22. Blasius B, Huppert A, Stone L, Complex dynamics and phase synchronization in spatially extended ecological systems, *Nature* **399**:354–359, 1999.
23. Kuske R, Gordillo LF, Greenwood P, Sustained oscillations via coherence resonance in SIR, *J Theor Biol* **245**:459–469, 2007.
24. Dushoff J, Plotkin JB, Levin SA, Earn DJD, Dynamical resonance can account for seasonality of influenza epidemics, *Proc Nat Acad Sci* **101**:16915–16916, 2004.